CONCLUSIONS

The main goal of this research study was to obtain chitosan/hydroxyapatite composites with higher sorption capacity using different types of hydroxyapatite. The results obtained showed that the morphological characteristics and sorption capacity of the composites depend on the type of hydroxyapatite used and the synthesis method. Thus, hexagonal well-formed crystallites, needle-like shape, cylindrical shape, lamellar elongated particles dispersed in amorphous polymer matrix were obtained. The calcination temperature at which the hydroxyapatite is obtained has a great influence on the porosity of the final materials.

The sorption capacity of chitosan/hydroxyapatite composites for Pb(II) ions from aqueous solutions ranged from 37.34 mg/g to 93.21 mg/g. These results indicated that the obtained composites have great potential as effective adsorbents for adsorption of lead ions from synthetic solutions and wastewater.

Also, their sorption capacity can be modulated by changing the synthesis method of hydroxyapatite.

REFERENCES

[1] Fu F., Wang Q., Removal of heavy metal ions from wastewaters: A review, Journal of Environmental Management .vol. 92, pp 407-418, 2011.

[2] Cho D.-W., Jeon B.-H, Chon C.-M., Kim Y., Schwartz F.W., Lee E.-S., Song H., A novel chitosan/clay/magnetite composite for adsorption of Cu(II) and As(V), Chemical Engineering Journal 200–202, pp 654–662, 2012.

[3] Wan Ngah W.S., Teong L.C., Hanafiah M.A.K.M., Adsorption of dyes and heavy metal ions by chitosan composites: A review, Carbohydrate Polymers 83, pp. 1446–1456, 2011.

[4] Pighinelli L., Kucharska M., Chitosan–hydroxyapatite composites, Carbohydrate Polymers 93, pp. 256–262, 2013.

[5] Bazargan-Lari R., Zafarani H.R., Bahrololoom M.E., Nemati A., Removal of Cu(II) ions from aqueous solutions by low-cost natural hydroxyapatite/chitosan composite: Equilibrium, kinetic and thermodynamic studies, Journal of the Taiwan Institute of Chemical Engineers 45, pp. 1642–1648, 2014.

[6] Li B., Shan C-L., Zhou Q., Fang Y., Wang Y.-L., Xu F., Han L-R., Ibrahim M., Guo L.-B., Xie G.-L., Sun G.-C., Synthesis, Characterization, and Antibacterial Activity of Cross-Linked Chitosan-Glutaraldehyde, Mar. Drugs 11, pp. 1534-1552, doi:10.3390/md11051534, 2013.

[7] Simonescu C.M., Melinescu A., Melinte I., Pătescu R.-E., Dragne M., Copper removal from synthetic aqueous solutions by hydroxyapatite granules synthesized using microwave heating, 15th International Multidisciplinary Scientific Geoconference SGEM2015, Ecology, Economics, Education and Legislation volume 1, pp. 177-184; 18-24 June 2015, Albena, Bulgaria ISBN 978-619-7105-39-1, DOI:10.5593/sgem2015B51.

FORMATION OF SILICON NANOSTRUCTURED SURFACE BY SELECTIVE CHEMICAL ETCHING

PhD M.T. Gabdullin

D.V. Ismailov

Zh.K. Kalkozova

A.B. Sagyndykov

Dr. Kh.A. Abdullin

Kazakh National University after al-Farabi, Almaty, **Kazakhstan**

ABSTRACT

Nanostructured surface of silicon wafers with low reflectivity was obtained in a two-stage process by selective chemical etching initiated by metal nanoclusters. Surface-enhanced Raman scattering (SERS) effect was observed on silicon substrates coated with silver nanoclusters at concentrations of test substance Rhodamine of ~10^{-12} M. It was shown that the depth of the structured layer is linearly dependent on the duration of the second stage etching up to etching time about 100 seconds. During the etching process, the formation rate of textured layer is twice faster in p-type silicon than in n-type silicon.

INTRODUCTION

The technology of obtaining nanostructured silicon surface is actively developed in the field of materials for renewable energy [1]. Surface of such silicon is textured in the form of nanoscale pillars. The texture leads to multiple reflection of light; as a result, the textured surface has very low reflectivity. Therefore it is possible to achieve a very low reflectance of light in the whole visible range that is important for solar cell (SC). It is important that the low reflection coefficient is achieved both at normal and inclined incidence of light [2]. Accordingly there is no need to create antireflection coatings of solar cells with nanostructured surface. Nanocrystalline silicon has a high optical absorption coefficient which allows to use thin silicon wafers and save silicon for manufacturing of solar cells that increases the economic efficiency of the solar cell production process.

Currently the SC-based nanostructured silicon passivated with conformal coating of aluminum oxide has demonstrated efficiency above 22% [3]. Nanostructured silicon also has a potential of practical application for creation of light-emitting devices [4], antibacterial coatings [5], gas sensors, sensors based on the effect of surface-enhanced Raman scattering (SERS) [6]. In recent years, active researches on production of

nanostructured silicon for solar cells and other device structures are being conducted. This paper presents the results on nanotexturing silicon surface with low reflectance for the creation of solar cells.

THE EXPERIMENTAL PART

We used polished plates of semiconductor silicon (ρ~5-15 Ω*cm) doped with boron (p-Si) or phosphorus (n-Si) as initial substrates. Before etching, the surface of silicon wafers was subjected to purification by boiling in acetone and ethanol followed by processing in a boiling aqueous solution of ammonium hydroxide and hydrogen peroxide, followed by rinsing in deionized water. Pre-cleaning of the silicon wafer surface provides the uniform formation of a subsequent texture [7-8].

At the first stage of chemical treatment, metal nanoparticles were formed on the surface of wafers; at the second stage selective etching of the silicon wafer surface initiated by metal clusters was carried out. Shallow diffusion p-n junctions were obtained using intense pulsed light annealing which was carried out in a 6 kW furnace with six linear halogen lamps. Time of heating up to 950°C was not more than 10 seconds.

The surface morphology of the samples was examined by scanning electron microscope (SEM) Quanta 200i 3D (FEI Company). Optical reflection spectra were measured by the UV-3600 spectrophotometer (Shimadzu), spectra of Raman scattering were measured by Raman NTEGRA SPECTRA microscope (NT-MDT) with the system of Raman scattering registration under excitation with a blue (473 nm) laser. Volt-ampere characteristics of the obtained structures in the dark and under illumination with a xenon lamp were measured using a P-30J potentiostat (Elins).

RESULTS AND DISCUSSION

The first stage of chemical treatment for creating the texture consisted of treating in aqueous solution of hydrofluoric acid and metal salt – silver nitrate, nitrate or copper chloride. The concentration of hydrofluoric acid solution, concentration of the metal salt, the treatment time were varied parameters.

In the case of the synthesis of silver particles, silicon wafers were first immersed in $H_2O+HF+AgNO_3$ solution on the first stage. H_2O:HF solutions with the ratio of 4:1 and with $AgNO_3$ concentration of 4, 6, 8 and 10 mmol were used during these experiments.

It was found that silver nanoparticles of spherical shape are formed on silicon substrate during the first 10-20 second. The shape of particles becomes elongated and the additional nanoparticles layers begin to form on the surface if the longer treatment at the first stage applied.

Fig. 1 and 2 show the surface morphology of the silicon after the first stage of the treatment in an aqueous solution of hydrofluoric acid with a concentration of silver nitrate of 8 mmol. Treatment was conducted for 10 seconds. It is evident that there are nanoparticles formed on the surface of silicon substrate. As can be seen in Fig. 1, particles with an average size of about 50-70 nm are arranged in a single layer on the substrate surface. The elemental analysis showed that they consist of silver.

a   b
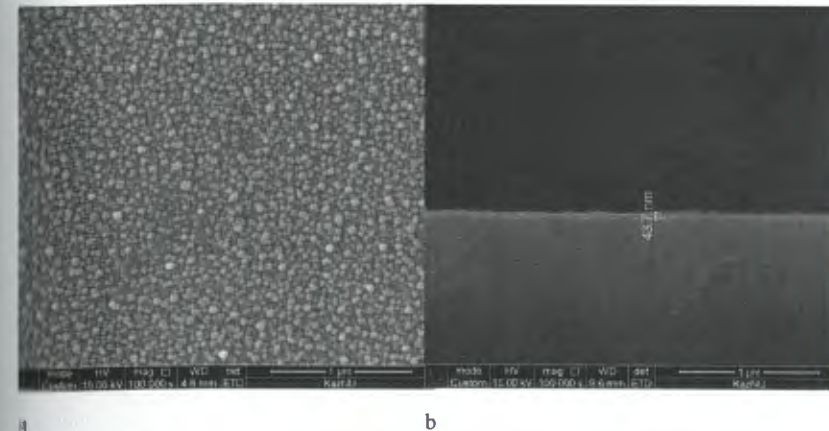
Figure 1. SEM image of Ag nanoparticles on the surface of silicon substrate (a) and cross-section SEM image of the sample (b).
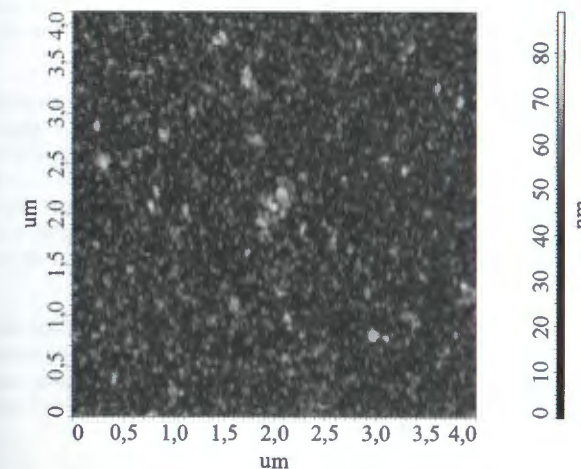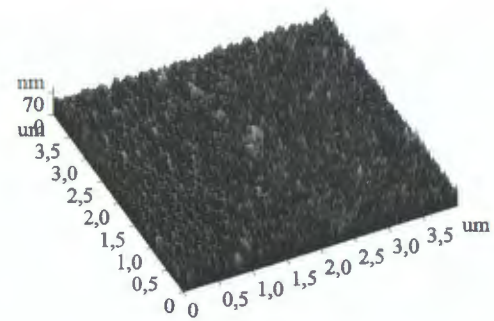
Figure 2. AFM images of Ag nanoparticles on the surface of silicon substrate.

In the case of creation of Si surface with copper clusters, solutions of cooper nitrate $H_2O+HF+Cu(NO_3)_2$ or cooper chloride ($H_2O+HF+CuCl_2$) were used, the ratio of water and hydrofluoric acid was 4:1, and the concentration of cooper salts was from 10 to 20 mM. The duration of treatment was from 20 to 100 sec. Similar with the case of silver nitrate, the formation of cooper nanoparticles on the silicon substrate surface takes place. The cooper particles have an average diameter of ~80-180 nm.

The silicon substrate surface on which the metal nanoparticles were deposited on the first stage of processing, can be used as substrate for detection of different organic molecules by the known effect of surface enhanced Raman scattering (SERS). It was found that the obtained silicon substrates with Ag and Cu nanoparticles on the surface demonstrate the considerable SERS effect when Rhodamine is used as a test substance. In the case of Si substrates with copper particles, appreciable SERS signal is observed at Rhodamine concentrations of 10^{-5} M, in the case of silver particles one can detect Rhodamine concentrations of 10^{-12} M.

To obtain silicon nanostructured surface, selective etching was carried out on the second stage of chemical treatment. The treatment of the silicon substrates with deposited metal nanoparticles by aqueous solution of hydrofluoric acid and hydrogen peroxide was applied. The treatment results in selective etching of silicon initiated by metal clusters. Usually solution $H_2O_2:HF:H_2O=1:2:10$ was used.

Figure 3a shows the surface morphology of the p-type silicon after two stages of processing. It is seen that two-stage treatment allow to obtain the substrate surface covered with columns with transverse dimensions of about 50-100 nm. Cross-section of the sample presented in Fig. 3b shows that the height of structured layer is about 300 nm.
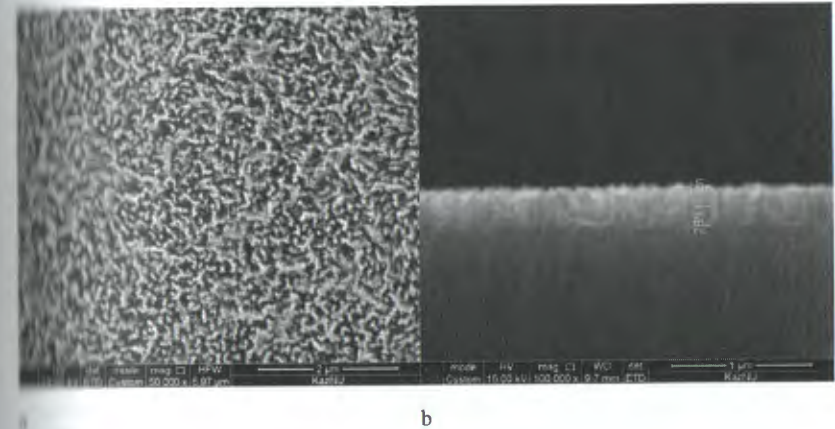
Figure 3. The surface morphology of the p-type silicon after two stages of processing (a), and cross-section of the sample (b).

Figure 4A shows the dependence of the average layer thickness of silver nanoparticles (1) after the first stage of processing within 20 seconds and thickness of the structured layer after the second processing stage (2) for 60 seconds on the concentration of silver nitrate in solution at the first stage of processing. It is seen that although a minimum average size of nanoparticles is obtained at AgNO3 concentration of 8 mmol, the concentration of $AgNO_3$ in the range of 4-8 mmol slightly changes the average particle size. The concentration of $AgNO_3$ above 10 mmol size leads to increase in the dimensions of the Ag particles.
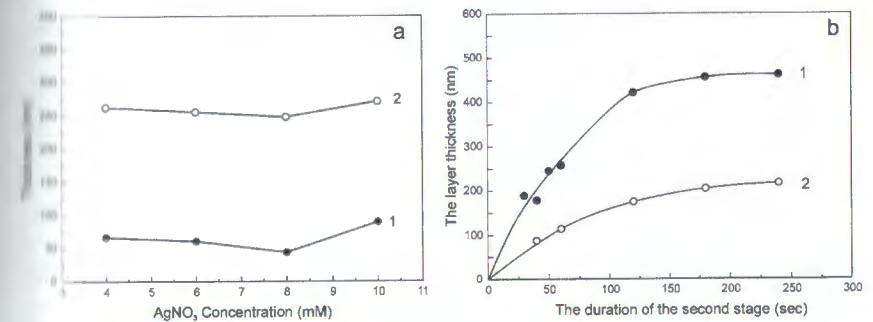
Figure 4. (a) Dependence of average thickness of nanoparticles layer after the first stage of treatment for 20 sec (1) and the thickness of the structured layer after the second stage of treatment for 60 seconds (2) on the concentration of $AgNO_3$ in the solution on

the first stage of treatment; (b) Dependence of the thickness of the structured layer in p-type (1) and n-type silicon (2) on the duration of the second stage of treatment.

Thickness of the structured layer obtained after second stage of processing slightly changes depending on size of particles if the duration of the second stage is fixed (Fig. 4a). This shows that the method of two-stage treatment is a proper way to obtain reproducible structured layer, because the result weakly depends on the concentration of silver salt and duration of the first stage. The main parameter determining the depth of structured layer is the duration of the second stage.

It is found that the depth of structured layer is approximately linearly dependent on duration of the second stage until ~100 sec, then the speed of the layer formation slows down. It can be seen from Fig. 4b, which shows the dependence of thickness of the structured layer in p-type silicon (curve 1) and n-type silicon (curve 2) on duration of the second stage treatment under the following processing options at the first stage: $AgNO_3$ concentration is 4 mmol, duration is 20 seconds. Since the parameters of nanoparticles weakly depend on the modes of processing in the first stage, as seen in Fig. 4a, similar dependencies of the structured layer depth from the etching at the second stage were also obtained in other modes of the first processing stage. The linear dependence of the structured layer depth on the duration of the second stage of processing allows adjusting the layer depth by selecting the duration of etching.

It can be seen from the comparison of etching speed of silicon of p-type and n-type with a resistivity of 5-15 Ω*cm under the same processing conditions (Fig. 4B) that the p-type silicon is etched about two times faster than the n-type silicon.

Silicon samples with a low coefficient of optical reflection were obtained after the second stage of processing using silver nanoparticles. Optical reflection spectra of samples in the range of 200-1000 nm exhibit a significant reduction in reflectance from ~30% to ~2-3% in all the above-mentioned wavelength range. Minimum reflection is achieved at the $AgNO_3$ concentration of 8 mmol, at duration of the first stage of 20 sec and the duration of the second stage of 60-120 sec.

In order to confirm the obtained results, SE samples with an area of 1-2 cm2 were made using the initial and textured silicon wafers. SE were obtained by means of fast diffusion using the surface source. A gel based on isopropyl alcohol, hydrochloric acid and tetraethoxysilane was made in order to obtain the diffusant. Boric acid (H3BO3) was added to the gel in the case of boron diffusion in n-Si, and orthophosphoric acid (H3PO4) was added to the gel for the diffusion of phosphorus in p-Si. The ratio of the basic and impurity components were varied. The gel was deposited on the Si wafers by spin-coating, then the wafers were dried and annealed at temperature of 950-1050oC during 20 sec.

Determination of effectiveness of the obtained SE was carried out under the illumination of halogen lamp. Current-voltage characteristics of the solar cells were measured in the dark and under illumination. Parameters obtained were compared with the current-voltage characteristic of the reference SE with known efficiency. Solar cells obtained from the initial and textured silicon have an efficiency of 10.5 and 11.2%

respectively. The fill factor of the SE based on textured silicon was less than the fill factor of the control sample due to the high serial resistance. More considerable increase in the efficiency of the textured SE can be achieved by optimizing the thickness of layer.

CONCLUSION

Nanostructured silicon wafers with low reflectivity was obtained in a two-stage process by selective chemical etching initiated by metal nanoclusters. The obtained silicon wafer surfaces demonstrate the reflectance of 2-3% in the visible range. Surface-enhanced Raman scattering (SERS) effect was observed on silicon substrates coated with silver or cooper nanoclusters. Test substance of Rhodamine can be detected up to concentration of ~10^{-12} M by using nanostructured silicon substrates covered with silver nanoparticles. Dependence of average thickness of nanoparticles layer after the first stage of treatment as well as the thickness of the structured layer after the second stage of treatment on the concentration of $AgNO_3$ in the solution was determined. It was shown that the depth of the structured layer is linearly dependent on the duration of the second stage etching up to etching time about 100 seconds. During the etching process, the formation rate of textured layer is twice faster in p-type silicon than in n-type silicon. Solar cells obtained from the initial and textured silicon have an efficiency of 10.5 and 11.2% respectively. Further increase of effectiveness of the textured SE can be achieved by optimizing the layer thickness.

REFERENCES

[1] Liu X., Coxon P.R., Peters M., Hoex B., Cole J.M., Fray D.J. Black silicon: fabrication methods, properties and solar energy applications //Energy&Environmental Science, vol. 7, pp 3223-3263, 2014.

[2] Wang H.P., Lin T.Y., Hsu C.W., Tsai M.L., Huang C.H., Wei W.R.,Huang M.Y., Chien Y.J., Yang P.C., Liu C.W., Chou L.J., HeJ.H. Realizing High-Efficiency Omnidirectional n-Type Si Solar Cells via the Hierarchical Architecture Concept with Radial Junctions// ACS Nano, vol.7, No.10, pp 9325–9335, 2013.

[3] Savin H., Repo P., Gastrow G., Ortega P., Calle E., Garín M., Alcubilla R. Black silicon solar cells with interdigitated back-contacts achieve 22.1% efficiency // Nature Nanotechnology, vol. 10, pp 624–628, 2015.

[4] Creazzo T., Redding B., Marchena E., Murakowski J., Prather D.W. Pulsed pumping of silicon nanocrystal light emitting devices //Optics Express. vol. 18, No. 11, pp 10924, 2010.

[5] Ivanova. E.P., Hasan J., Webb H.K., Gervinskas G., Juodkazis S., Truong V.K., Wu A.H., Lamb R.N., Baulin V.A., Watson G.S., Watson J.A., Mainwaring D.E., Crawford R.J. Bactericidal activity of black silicon// Nat Commun. 4:2838. doi: 10.1038/ncomms3838, 2013.

[6] Deng Y.L., JuangY.J. Black silicon SERS substrate: Effect of surface morphology on SERS detection and application of single algal cell analysis//Biosensors and Bioelectronics, vol. 53, pp 37–42, 2014.

[7] Peng K., Wu Y., Fang H., Zhong X., Xu Y., Zhu J. Uniform, Axial-orientation alignment of one- dimensional single-crystal silicon nanostructure arrays // Angewandte Chemie International Edition, vol. 44. pp 2797 – 2802, 2005.

[8] Peng K.Q., Hu J.J., Yan Y.J., Fang H., Xu Y., Lee S.T., Zhu J. Fabrication of single crystalline silicon nanowires by scratching a silicon surface with catalytic metal particles //Advanced Functional Materials, vol 16. pp 387 – 94, 2006.

HEAT EXCHANGE FEATURES IN THE MICRO SYSTEM ELEMENTS OF FUNCTIONAL PURPOSE WITH THE ENVIRONMENT

Ph.D. Sergey Evstafye

Prof. Natalia Korobova

Prof. Vyacheslav Samoilykov,

Prof. Sergey Timoshenkov

National Research University of Electronic Technology (MIET), **Russia**

ABSTRACT

The macroscopic equations applicability of thermo fluid dynamics for calculation of heat transfer elements in Microsystems has been discussed. The assessment of spatial and temporal scales that determine applicability limits of the above equations was based on the experimental data analysis. It was shown that the characteristic size greater than 0.1 microns and time interval larger than 10^{-9} seconds can be used in the "classic" regularities with the correction introduction. It was necessary to use statistical methods for calculating upon exceeding the specified spatial and temporal scales.

Keywords: Microsystems, technology, heat transfer, thermodynamics, method

INTRODUCTION

Currently, micro system technology (MST) is one of the fastest developing science and technology areas. Well mastered technology of integrated circuits (ICs) manufacturing, and a great need for small and energy-efficient devices for various functional applications has been contributed to the rapid MST growth. Microelectronic technology has allowed exactly implementing a set of elements that were impossible to produce using macro-technologies. Typical dimensions of the MST elements (L_x) are in the range of 0.5 - 100 microns that substantially (by orders of magnitude) different from the typical macro sizes. In general, as the characteristic size of the active MST element L_x may be ratio of element volume V to the bounding surface S, that is $L_x = V / F$.

The control action on the active element structure (node) is accompanied, as a rule, by the heat, requiring subsequent scattering. Heat dissipation occurs in equilibrium (relatively slow) conditions, when we have the characteristic size of the active elements. In this case, it can be successfully used the well-known macrocosm physical laws. However, increasing the speed of active structures requires a reduction in their size, which changes the nature of heat, moving it away from equilibrium. This fact is directly related to the increasing role of the phenomena occurring on the surface, compared with the phenomena occurring in the volume. Thus, the factor of "characteristic dimension" is becoming increasingly important in the transition to the micro- and nanoscale. The tendency to minimize the size of the MST elements requires very specific methods of experimental studies, which greatly limits their use. Therefore the methods of

16th INTERNATIONAL MULTIDISCIPLINARY SCIENTIFIC GEOCONFERENCE
SGEM 2016

**NANO, BIO AND GREEN – TECHNOLOGIES
FOR A SUSTAINABLE FUTURE
CONFERENCE PROCEEDINGS
VOLUME I**

- - - - - - - - - - - - - - - - - -

MICRO AND NANO TECHNOLOGIES,

ADVANCES IN BIOTECHNOLOGY

- - - - - - - - - - - - - - - - - -

30 June – 6 July, 2016
Albena, Bulgaria

ORGANIZERS AND SCIENTIFIC PARTNERS

- BULGARIAN ACADEMY OF SCIENCES
- ACADEMY OF SCIENCES OF THE CZECH REPUBLIC
- LATVIAN ACADEMY OF SCIENCES
- POLISH ACADEMY OF SCIENCES
- RUSSIAN ACADEMY OF SCIENCES
- SERBIAN ACADEMY OF SCIENCES AND ARTS
- SLOVAK ACADEMY OF SCIENCES
- NATIONAL ACADEMY OF SCIENCES OF UKRAINE
- INSTITUTE OF WATER PROBLEM AND HYDROPOWER OF NAS KR
- NATIONAL ACADEMY OF SCIENCES OF ARMENIA
- SCIENCE COUNCIL OF JAPAN
- THE WORLD ACADEMY OF SCIENCES (TWAS)
- EUROPEAN ACADEMY OF SCIENCES, ARTS AND LETTERS
- ACADEMY OF SCIENCES OF MOLDOVA
- MONTENEGRIN ACADEMY OF SCIENCES AND ARTS
- CROATIAN ACADEMY OF SCIENCES AND ARTS, CROATIA
- GEORGIAN NATIONAL ACADEMY OF SCIENCES
- ACADEMY OF FINE ARTS AND DESIGN IN BRATISLAVA
- TURKISH ACADEMY OF SCIENCES
- BULGARIAN INDUSTRIAL ASSOCIATION
- BULGARIAN MINISTRY OF ENVIRONMENT AND WATER

HONORED ORGANIZER

BULGARIAN ACADEMY OF SCIENCES

EXCLUSIVE SUPPORTING PARTNER

YOUR SPA & Albena
WELLNESS DESTINATION

INTERNATIONAL SCIENTIFIC COMMITTEE
Nano, Bio and Green – Technologies for a Sustainable Future

- PROF. STEFAN DIMOV, UK
- PROF. MARIAPIA VIOLA MAGNI, ITALY
- PROF. STEFFEN LEHMANN, AUSTRALIA